Chinese Journal of Polymer Science Vol. 31, No. 3, (2013), 514–520

Chinese Journal of Polymer Science
© Chinese Chemical Society
Institute of Chemistry, CAS
Springer-Verlag Berlin Heidelberg 2013

SIMULATION OF ELECTRICAL FIELD FOR THE FORMATION MECHANISM OF BIRD'S NEST PATTERNED STRUCTURES BY ELECTROSPINNING*

Xiang-yu Ye[a], Yi-ning Jin[a], Xiao-jun Huang[a], Lei Luo[b] and Zhi-kang Xu[a**]

[a] *MOE Key Laboratory of Macromolecular Synthesis and Functionalization, Department of Polymer Science and Engineering, Zhejiang University, Hangzhou 310027, China*

[b] *Institute of Advanced Digital Technology and Instrument, Zhejiang University, Hangzhou 310027, China*

Abstract In our previous work, it was found that large Bird's Nest patterned nanofibrous membranes can be simply electrospun from chlorinated polypropylene solution doped with an ionic liquid, and a plausible formation mechanism of Bird's Nest patterned architectures was proposed. Here, we use Ansoft Maxwell version 12 software (3D, electrostatic solver) to simulate the electrical field distribution of the electrospinning setup, and to clarify the rationality of proposed formation mechanism. Calculation results clearly show that the introduction of charged nanofibrous bundles would produce a similar patterned electrical field distribution, which definitely confirms the important role of surface residual charges. The proposed mechanism can be well extended to other polymer systems including polystyrene, poly(acrylonitrile-*co*-acrylic acid) and chitosan/poly(ethylene oxide).

Keywords: Electrospinning; Patterned structures; Finite element analysis; Electrical field; Theoretical simulation.

INTRODUCTION

Electrospinning has been extensively studied as a versatile laboratory method for preparing continuous nanofibers from polymers and ceramics in recent years[1]. The electrospun nanofibers are usually collected as randomly overlapped structures due to their inherent chaotic nature of bending instability[2]. The so-called nonwoven meshes are of great interest for applications including high-flux filtration[3], waste-water treatment[4], affinity membrane chromatography[5], enzyme immobilization[6], and so on. However, for micro-device fabrications[7] or tissue regeneration[8] that often requires well-aligned and highly ordered architectures, it is necessary to control the spatial orientation or deposition of the nanofibers.

Enormous efforts have been made to overcome the challenge, and some success has been achieved so far. For example, by using rings as auxiliary electrodes, it was possible to control or eliminate the whipping instability in conventional electrospinning experiments and control the deposition of electrospun nanofibers[9]. Zhang *et al.* found that a patterned structure similar to the patterned conductive woven wire collector was generated and most of the fibers deposited directly on the wires[10]. The orientation of the fibers was affected by the diameter of the wires, and the protrusions in the collector were very important parameters. Xia *et al.* reported that nanofibers can be uniaxially aligned by introducing an insulating gap into the conductive collector, and the effects of the area and geometric shape of the gap on the deposition behavior were systematically studied[11].

* This work was financially supported by the National Natural Science Foundation of China (No. 50933006) and Zhejiang Provincial Innovative Research Team (No. 2009R50004).

** Corresponding author: Zhi-kang Xu (徐志康), E-mail: xuzk@zju.edu.cn

Reveived June 18, 2012; Revised September 26, 2012; Accepted September 27, 2012
doi: 10.1007/s10118-013-1238-3

Theoretical simulations revealed that the horizontal electrical field strength E_x is a key factor in stretching electrospun jet across the gap and eventually forming aligned nanofibers[12]. More recently, Ziaie *et al.* showed a novel electrospinning technique called 'field-enhanced electrospinning' for selective deposition of nanofibers on an elastomeric substrate with gold-coated pyramidal protrusions[13]. This method provided small feature dimensions (8 μm × 8 μm) over a 5 mm × 10 mm area. The key points of all the above mentioned methods are to manipulate the electrical field distribution and control the jet travelling path[14]. However, such approaches require exquisite laboratory procedures or specially designed collectors, and face the massive preparation problem.

In our previous work, we found that large Bird's Nest patterned nanofibrous membranes can be simply electrospun from chlorinated polypropylene and polystyrene in xylene/cyclohexanone (1:1, *V*/*V*) solutions doped with an ionic liquid under appropriate conditions[15]. We carefully evaluated the effects of different operating parameters on the surface morphology changes of as-spun nanofibrous membranes. Preliminarily results suggest the electrostatic repulsion interactions between the residual surface charges and the upcoming fibers play a key role, but such conclusion lacks theoretical foundation. Here, we use finite element analysis method to simulate the electrical field distribution of the electrospinning setup and try to reveal insights into the formation mechanism of such Bird's Nest patterned structures. Further, we also want to figure out whether such mechanism can be well extended to other polymer systems.

EXPERIMENTAL

Chlorinated polypropylene (CPP, 30 wt% chlorinated degree, $M_n = 1.08 \times 10^5$) was purchased from Hangzhou Juli Chemical Co., Ltd. Polystyrene (PS, $M_n = 8.13 \times 10^4$) was got from Zhenjiang Chi Mei Chemical Co., Ltd. Poly(acrylonitrile-*co*-acrylic acid) (PANCAA, acrylic acid 10%, $M_\eta = 7.80 \times 10^4$) was synthesized by a water phase precipitation copolymerization process according to our previous work[4]. Chitosan (CS, degree of deacetylation 90%, $M_n = 1.0 \times 10^5$) was bought from Weifang Sea Source Biological Products Co., Ltd. Poly(ethylene oxide) (PEO, $M_n = 1.0 \times 10^7$) was supplied by Sigma-Aldrich. 1-Dodecyl-3-methylimidazolium hexafluorophosphate [C12Mim][PF6] (purity > 95%) was a commercial product from Lanzhou Greenchem ILS, LICP, CAS and used without further treatment. Xylene, cyclohexanone, *N*,*N*′-dimethylformamide and acetic acid were of analytical grade and used as received.

For CPP and PS solutions, xylene/cyclohexanone (1:1, *V*/*V*) mixed solvent was used, and the polymer concentration and [C12Mim][PF6] content were 180 g/L and 18 g/L. The concentration of PANCAA in DMF was 20 g/L. CS/PEO blend aqueous solution was prepared. First, chitosan was dissolved in 50 vol% acetic acid at room temperature to form a 15 g/L solution. At the same time, 40 g/L PEO aqueous solution was ready. Then, the CS solution and PEO solution were mixed in a weight ratio of 85:15. After degassing completely, electrospinning was performed using a 20 mL syringe with a 1.2 mm diameter stainless steel needle. The tip-to-collector distance was fixed at 15 cm and collection time was 20 min for all samples. Other conditions were as follows: CPP and PS solutions, 9.5 kV, 0.5 mL/h; PANCAA solution, 14 kV, 1.0 mL/h; CS/PEO blend solution, 8 kV, 0.3 mL/h. The electrospinning process was conducted in an enclosed chamber, and the relative humidity was set at 50%. Surface morphologies of the samples were studied by field emission scanning electron microscopy (FESEM, SIRION-100, FEI, USA) after sputtering coated with gold.

Ansoft Maxwell version 12 software (3D, electrostatic solver) was applied to simulate the electrical field distribution. The model was built based on the real operating parameters. For simple electrospinning system: a 1 cm long solid stainless steel needle with 1.2 mm diameter was used and the excitation voltage was 9.5 kV; the tip-to-collector distance was 15 cm; a 10 cm × 10 cm × 1 mm aluminum collector was used and the excitation voltage was 0 kV as it was grounded; the region material was assigned as air. For the charged patterned and randomly overlapped bundles systems: the length and diameter of the bundles were set as 400 μm and 2 μm, polystyrene was selected from the software installed material database as the model material, and the excitation voltage was 0.2 kV (according to reference 13); a 1 mm × 1 mm × 1 mm small aluminum collector was placed

75 μm below the bundles and the excitation voltage was 0 kV; the region material was assigned as air. The calculated results had an acceptable error percentage of 1%.

RESULTS AND DISCUSSION

When electrospun chlorinated polypropylene and polystyrene solutions doped with [C12Mim][PF6], as can be seen from Fig. 1, we surprisingly found that micron dimension (20–200 μm) Beijing National Stadium — 'Bird's Nest' like 3D patterned nanofibrous mats can be directly obtained just by using a conventional electrospinning setup[15]. Therefore, we systematically studied the effects of various parameters, including solution viscosity, conductivity, collection time, relative humidity, applied voltage and collector design, on the surface morphology of the as-spun nanofibrous membrane, and it was demonstrated that those factors which enhanced surface charge accumulation would promote the formation of patterned structures, and vice-versa. The nest walls are composed of nanofibrous bundles resulting from a 'backbuilding' process, which has been proved by the appearance of conjoined and twisted nanofibers: negative charge is drawn back through the positively charged jet, so that these nanofiber segments begin to have excess negative charge; those segments closer to the needle with excess positive charge are drawn first towards the negatively charged nanofiber segments before hitting the collector as the collector repels them at the same time[15]. The bundles would build up large amount of electrostatic charges[16], as Patra *et al.* reported that even polyacrylonitrile fibers had a charge density of 30–50 nC/mg[17]. To sum up all the experiment results, we proposed a plausible formation mechanism of Bird's Nest patterned architectures: nanofibrous bundles are first aggregated by a 'backbuilding' process with charge accumulation; then the formation of the bird's nest patterns resulted from the electrostatic repulsion between the residual surface charges of as-prepared membrane and the upcoming fibers. However, the exact role of residual surface charges is still unaware and whether the formation mechanism works for other polymers needs further consideration.

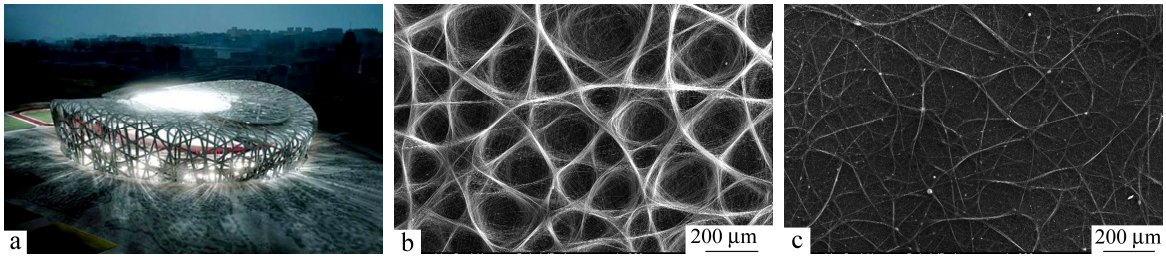


Fig. 1 Photographs of (a) Beijing National Stadium — Bird's Nest, (b) chlorinated polypropylene nanofibrous membrane with patterned structure and (c) polystyrene nanofibrous membrane with patterned structure

At first we found that it is unable to get similar patterned structures from 100 g/L PANCAA/DMF solution in any electrospinning condition, and we ascribe this to the polar property of PANCAA which would greatly limit the charge accumulation. Nevertheless, when the solution concentration was reduced to 20 g/L, the electrospun nanofibrous membranes showed patterned structures with serious beaded-bundles (Figs. 2a, 2c). These structures should result from the low solution viscosity (insufficient chain entanglement)[18], and the beaded-bundles carried a large amount of charges and accumulated quickly[19]. To validate this hypothesis, we electrospun chitosan a typical kind of polycations, one characteristic of which is the gelation usually occurs at low concentration with insufficient chain entanglement density[20]. Certain amount of PEO solution was added in chitosan solution to facilitate the electrospinning process. As expected, the resultant nanofibrous membranes formed patterned structures again with serious beaded-bundles (Figs. 2b, 2d). We note that some authors had published 'dimpled' or 'honeycomb' structures which are a little parallelism to our nest structures, including PEO[19], polycaprolactone (PCL)[21], polyurethane (PU)[22], polyacrylonitrile (PAN), poly(vinyl alcohol) (PVA) and PEO[23]. One of the common features for the mentioned work is that the authors used polar polymers and

serious beaded-bundles usually formed. The formation process of beaded-bundles can be described as follows: because of the high voltage, fast spinning rate or insufficient chain entanglement, the electrospun fibers are arriving at the collector wet and full of beaded defects[19]. These beads and fibers adhere to each other through surface tension and electrostatic repulsion[23], and form a thick, continuous layer of polymer particles (beaded-bundles) that eventually build up enough electrostatic charges. In short, the formation of Bird's Nest patterned architectures is a general phenomenon, non-polar polymers or polar polymers can all be electrospun into patterned structures as long as charged nanofibrous bundles or charged beaded-bundles form. Such exciting results further drive us to study the formation mechanism theoretically to figure out the underlying principles.

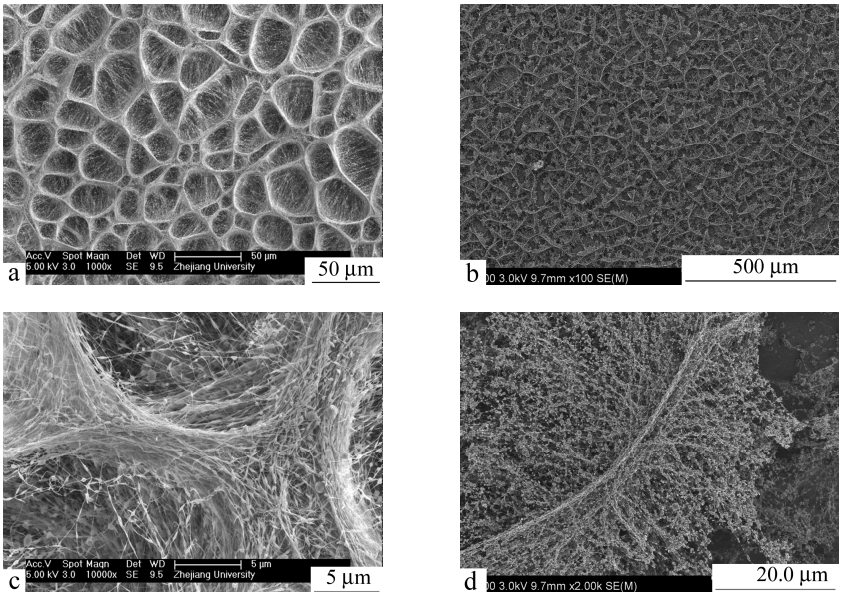


Fig. 2 SEM pictures of (a) poly(acrylonitrile-*co*-acrylic acid), (b) chitosan/poly(ethylene oxide) nanofibrous membranes with patterned structures and (c, d) close-up view of the bundles of (a, b)

The deposition behavior of nanofibers is mainly determined by the electrical field distribution, which would further determine the polymer jet travelling path from the needle to the collector. Finite element analysis method is usually applied to simulate the electrical field[24]. Various softwares such as COMSOL 3.4[13], Ansys[25], Students's Quick Field Program[26], Matlab and CFD-ACE[27] had been used and satisfactory simulation results were got. The calculated electrical field distribution shows good agreement with the experimental results and can be used to predict the jet deposition behavior. Here, we used Ansoft Maxwell version 12 (3D, electrostatic solver) to simulate the electrical field distribution. One biggest advantage of this software is its automatic adaptive meshing function, one only need specify geometry, material properties and desired output. Ansoft Maxwell will automatically generate an appropriate, efficient and accurate mesh for solving the problem. This proven automatic adaptive meshing process removes complexity from the analysis process and allows you to benefit from a highly efficient, easy-to-use design flow. In the calculated figures, the colors imply the magnitude value while the arrows indicate the direction of the electrostatic field lines. First, simple electrospinning system was simulated. As shown in Fig. 3(a), the voltage decreases from the needle to the collector, yet as approaching the collector, the voltage tends to be uniform at the same height. The electrical field distribution shows a similar form (Fig. 3b). We can clearly see from the side view of electrical field simulation results (Fig. 3c) that as away from the needle, the electrical field lines are perpendicular to the collector and evenly distribute. These features can be used to explain why the nanofibers are randomly and uniformly deposited. Our results are consistent with previous simulation work[9] and agree with experimental data, which demonstrates the validity of established model and method.

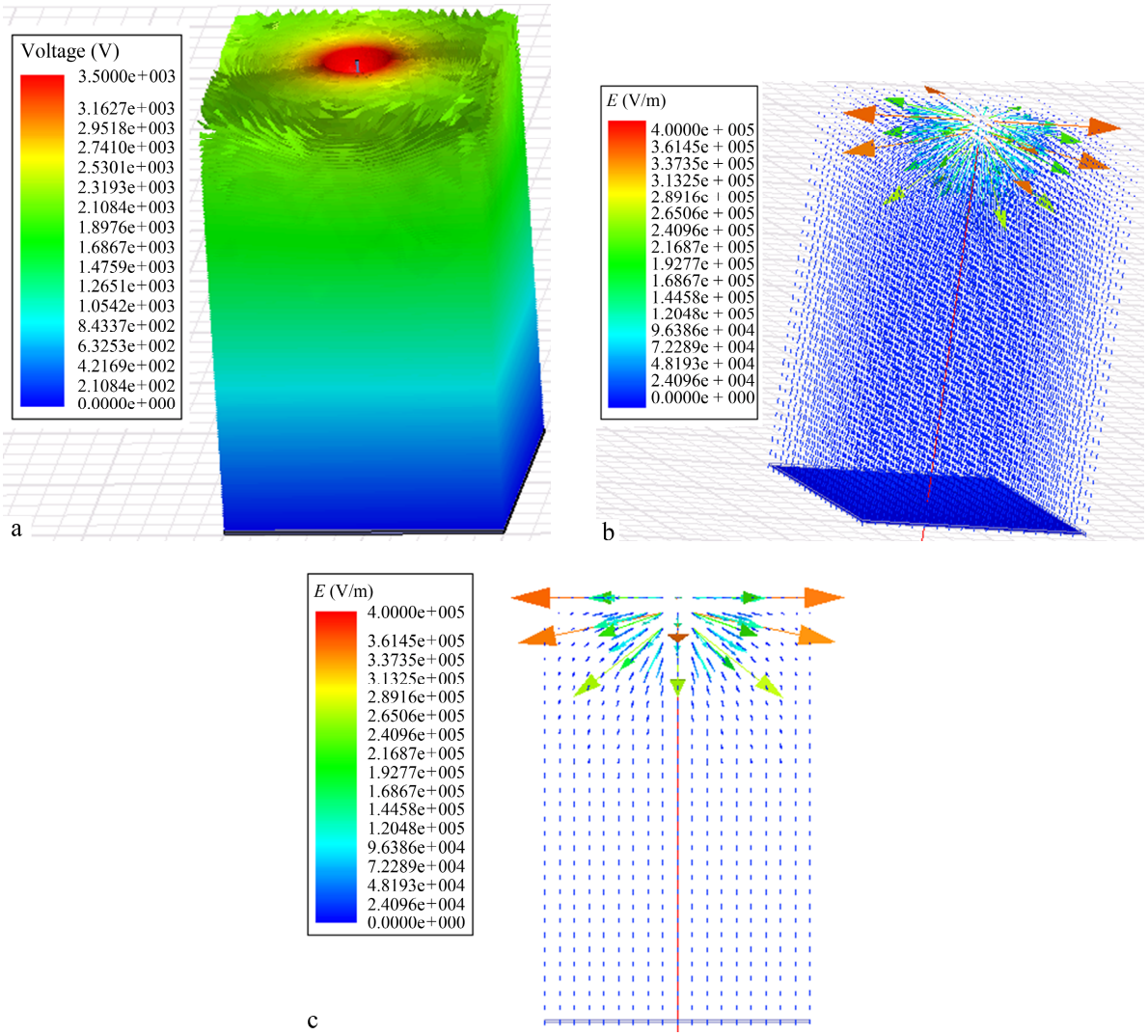


Fig. 3 (a, b) Voltage and electrical field distributions in the region between the needle and the collector and (c) side-view of the electrical field vectors

It ended in failure for attempts to simulate the real electrospinning setup with small charged bundles, because the size of the bundles is smaller than the self-adaptive mesh size of the collector. Reducing the mesh size to the micronmeter range means enormous running time. Furthermore, the meshing process uses a highly robust volumetric technique, and small mesh would exceed the computational capabilities. Theoretically, electrical field is a vector and the sum of different vector components at a certain point. Thus, the electrical field near the collector should be the sum of the electrical field exerted by the needle and charged bundles. Considering that the electrical field of the needle is uniformly distributed, the electrical field distribution near the collector is mainly determined by the electrical field of the charged bundles. Therefore, we simulated the electrical field distribution of the charged bundles.

The electrical fields of patterned and randomly overlapped charged bundles systems were both simulated. The model was setup according to the real situation: the length and diameter of the bundles were set as 400 μm and 2 μm; polystyrene was set as the bundle material; the excitation voltage was set as 0.2 kV[13]; a small aluminum collector was placed 75 μm below the bundles and the excitation voltage was set as 0 kV. As shown in Fig. 4, a similar patterned electrical field distribution was achieved, where the strength of electrical field

decreases away from the bundles. The charged bundles would prevent new electrospun fibers from laying directly on the as-spun nanofibrous membrane[19]. Instead they would suspend slight above the surface, and a reversely patterned structures formed. From that perspective, our simulation results clearly prove the important role of residual surface charges and the rationality of our previous proposed formation mechanism.

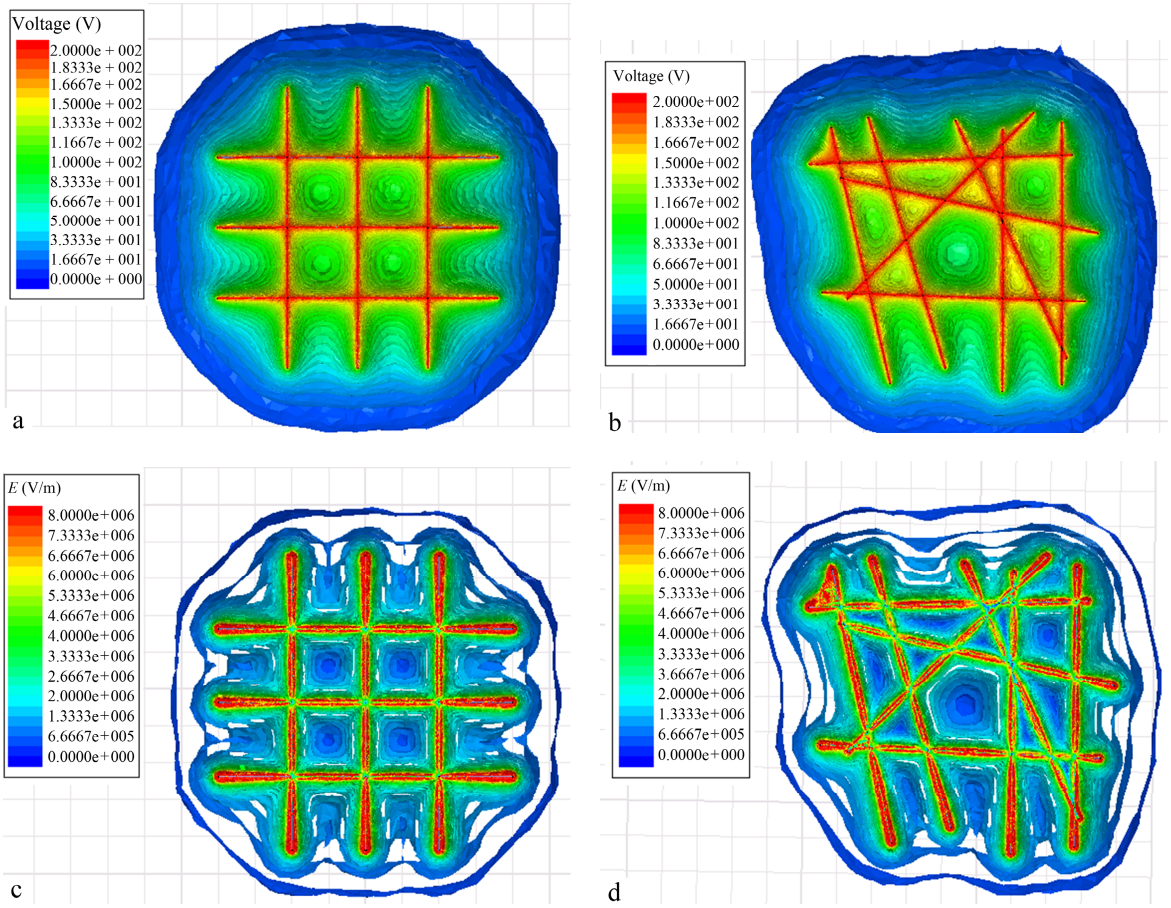


Fig. 4 Calculated voltage (a, b) and electrical field distribution (c, d) near the charged patterned and randomly overlapped bundles

CONCLUSIONS

In summary, we find that the formation of Bird's Nest patterned architectures by electrospinning is a general phenomenon. It works well with non-polar polymers like chlorinated polypropylene and polystyrene, and polar polymers like poly(acrylonitrile-*co*-acrylic acid) and chitosan/poly(ethylene oxide) as long as the charged bundles form by selecting appropriate operating parameters. To theoretically figure out the formation mechanism of patterned structures, finite element analysis method using Ansoft Maxwell version 12 software (3D, electrostatic solver) was applied to simulate the electrical field distribution of the electrospinning setup. Calculation results clearly show that the introduction of charged nanofibrous bundles would produce a similar patterned electrical field distribution, which definitely confirms the important role of surface residual charges. We believe our work opens a new avenue for the preparation of patterned structures, and such patterned nanofibrous membrane may find potential applications for air filtration and tissue regeneration scaffolds.

REFERENCES

1 Huang, Z.M., Zhang, Y.Z., Kotaki, M. and Ramakrishna, S., Compos. Sci. Technol., 2003, 63: 2223
2 Li, D., Wang, Y.L. and Xia, Y.N., Nano. Lett., 2003, 9: 1167
3 Yoon, K., Kim, K., Wang, X.F., Fang, D.F., Hsiao, B.S. and Chu, B., Polymer, 2006, 47: 2434
4 Ye, X.Y., Liu, Z.M., Wang, Z.G., Huang, X.J. and Xu, Z.K., Mater. Lett., 2009, 63: 1810
5 Che, A.F., Huang, X.J. and Xu, Z.K., J. Membr. Sci., 2011, 366: 272
6 Wang, Z.G., Wan, L.S., Liu, Z.M., Huang, X.J. and Xu, Z.K., J. Mol. Cat. B: Enzym., 2009, 56: 189
7 Huang, Y., Duan, X.F., Wei, Q.Q. and Lieber, C.M., Science, 2001, 291: 630
8 Ye, L., Wu, X., Geng, X., Duan, Y.H., Gu, Y.Q., Zhang, A.Y., Zhang, J. and Feng, Z.G., Chinese J. Polym. Sci., 2010, 28(5): 829
9 Deitzel, J.M., Kleinmeyer, J., Hirvonen, J.K. and Tan, N.C.B., Polymer, 2001, 42: 8163
10 Zhang, D.M. and Chang, J., Adv. Mat., 2007, 19: 3664
11 Li, D., Ouyang, G., McCann, J.T. and Xia, Y.N., Nano. Lett., 2005, 5: 913
12 Yan, H., Liu, L.Q. and Zhang, Z., Appl. Phys. Lett., 2009, 95: 143114
13 Ding, Z.W., Salim, A. and Ziaie, B., Langmuir, 2009, 25: 9648
14 Teo, W.E. and Ramakrishna, S., Nanotechnology, 2006, 17: R89
15 Ye, X.Y., Huang, X.J. and Xu, Z.K., Chinese J. Polym. Sci., 2012, 30(1): 130
16 Theron, S.A., Zussman, E. and Yarin, A.L., Polymer, 2004, 45: 2017
17 Kalayci, V.E., Patra, P.K., Kim, Y.K., Ugbolue, S.C. and Warner, S.B., Polymer, 2005, 46: 7191
18 Mckee, M.G., Wilkes, G.L., Colby, R.H. and Long, T.E., Macromolecules, 2004, 37: 1760
19 Deitzel, J.M., Kleinmeyer, J., Harris, D. and Tan, N.C.B., Polymer, 2001, 42: 261
20 Kim, T.G., Chung, H.J. and Park, T.G., Acta Biomat., 2008, 4: 1611
21 Ramakrishna, S., Fujihara, K., Teo, W.E., Lim, T.C. and Ma, Z.W., "An introduction to electrospinning and nanofibers", World Scientific, Singapore, 2005, p. 109
22 Thandavamoorthy, S., Gopinath, N. and Ramkumar, S.S., J. Appl. Polym. Sci., 2006, 101: 3121
23 Yan, G.D., Yu, J., Qiu, Y.J., Yi, X.H., Lu, J., Zhou, X.S. and Bai, X.D., Langmuir, 2011, 27: 4285
24 Wang, Y.Z., Li, H., Wang, G.X., Yin, T.Y., Wang, B.C. and Yu, Q.S., J. Nanosci. Nanotech., 2010, 10: 1699
25 Li, W.W., Zheng, G.F., Wang, X., Wang, H. and Sun, D.H., Proceedings of the 2010 5th IEEE International Conference on Nano/Micro Engineered and Molecular Systems., IEEE Xplore, New York, p. 483
26 Li, D., Wang, Y.L. and Xia, Y.N., Nano. Lett., 2003, 9: 1167
27 Chaurey, V., Chiang, P.C., Polance, C., Su, Y.H., Chou, C.F. and Swami, N.S., Langmuir, 2010, 26: 19022